ADVANCED FUNCTIONAL MATERIALS

DOI: 10.1002/adfm.200601174

Catalytic Performance of Nanoscale-Corrugated Gold and Silver Films for Surface-Enhanced Chemiluminescence**

By *Meigui Ou*, *Guowei Lu*, *Hong Shen*, *Armel Descamps*, *Christophe André Marquette*, *Loïc Jacques Blum*, *Gilles Ledoux*, *Stéphane Roux*, *Olivier Tillement*, *Bolin Cheng*, and *Pascal Perriat**

Biochips of corrugated gold and silver displaying surface plasmon resonance at different energies are fabricated to determine the nature of the mechanism responsible for the surface-enhanced chemiluminescence (SECL) of luminol. This Full Paper proves that, whereas silver possesses the strongest resonance and the greatest plasmon overlap with luminol emission, silver is also the metal that induces the lowest CL enhancement (two orders of magnitude less than gold). Therefore, the enhancement mechanism is not related to plasmon-assisted processes but rather originates from catalytic properties induced by corrugation of the metal film.

1. Introduction

Among the numerous surface-enhanced (SE) phenomena that have been studied in the past decades (SE Raman scattering, SE fluorescence), SE chemiluminescence (SECL) is the most recent one that has been investigated. It was reported for differently colored CL reagents near silver particles[1] or surfaces[2] and for luminol near gold particles[3] or corrugated films.[4] Two mechanisms are known to contribute to SE Raman scattering (SERS): an increase of the local electromagnetic field[5] and an electronic interaction between the metal and adsorbate, that is, a "chemical" effect.[6] The mechanisms responsible for SECL are still unknown and, according to the authors, they could be, similar to SERS, related to either a plasmonic enhancement[1] or a catalytic effect.[3] The plasmon-assisted enhancement arises from an overlap between the emission of the CL agent and the surface plasmon resonance (SPR) of the supporting metal; promoted by the excitation of surface plasmons in the metal and by a modification in the photonic mode density,[7] it would yield a strong increase in the low quantum efficiency of the CL agent. The catalytic effect should be facilitated by the generation of radicals and some electron-transfer processes on the surface of the metal particles. This Full Paper aims to prove the nature of the mechanism really involved in SECL by studying the luminol–hydrogen peroxide CL, which is one of the most sensitive CL reactions. This is done by thoroughly investigating the CL enhancement obtained at the vicinity of the corrugated metal films on which horseradish peroxidase (a catalyser of luminol CL) has been fixed via a biotinylated peptide (Fig. 1). In the experiments presented, the chemical nature of the metal (Au, Ag, or AuAg alloy) and the overlap between luminol emission and plasmon absorption were varied independently. For a better understanding of the mechanisms involved, the distance between metal and peroxidase has also been varied in a systematic and quantitative way via intermediate peptides with different lengths. It will be shown that the enhancement observed is entirely due to the catalytic efficiency induced by metal corrugation.

2. Results and Discussion

Figure 2 shows the versatility of the pulsed-laser deposition technique used for depositing films with a nominal thickness of about 25 nm onto a fused quartz substrate.[8] As evidenced by the atomic force microscopy (AFM) images on the left of Figure 2, this technique allows either flat, "bulklike" films, presenting the main features of gold bulk absorption (Fig. 3b), or rough, "clusterlike" films, presenting a localized SPR peak (Fig. 2, right), to be obtained.[4] The plasmon position of the island films undergoes a red-shift compared to free clusters[9]

[*] Prof. P. Perriat, M. G. Ou, A. Descamps
Groupe d'Étude de Métallurgie Physique et de Physique des Matériaux
INSA de Lyon
69621 Villeurbanne Cedex (France)
E-mail: pascal.perriat@insa-lyon.fr
Dr. G. W. Lu, Dr. H. Shen, Prof. B. L. Cheng
Beijing National Laboratory for Condensed Matter Physics
Institute of Physics, Chinese Academy of Sciences
Beijing 100080 (P.R. China)
Dr. C. A. Marquette, Prof. L. J. Blum
Laboratoire de Génie Enzymatique et Biomoléculaire
Université Claude Bernard Lyon I
69622 Villeurbanne Cedex (France)
Dr. G. Ledoux, Dr. S. Roux, Prof. O. Tillement
Laboratoire de Physico-Chimie des Matériaux Luminescents
Université Claude Bernard Lyon I
69622 Villeurbanne Cedex (France)

[**] This work was financially supported by the National Natural Science Fundation of China (Grant no. 10574157), the National Basic Research Program of China (Grant no. 2006cb302900), and the AFCRST of France. Supporting Information is available online from Wiley InterScience or from the author.

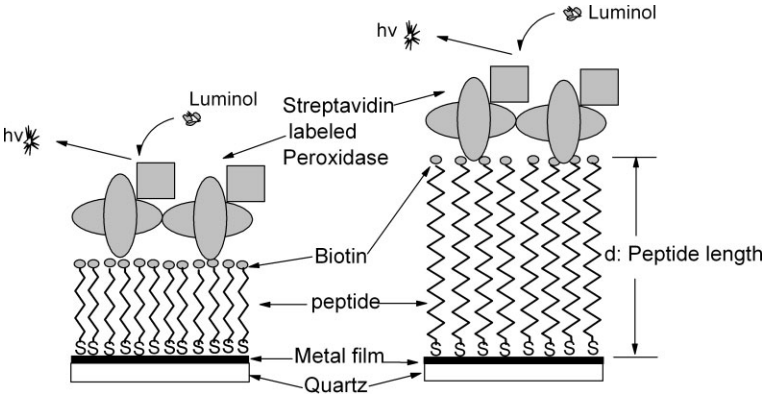

Figure 1. Schematic representation of the process involved in luminol chemiluminescence catalyzed by peroxidase fixed at the metal surface.

and can be adjusted simply by varying the glass-substrate temperature during deposition (Table 1). For all the compositions studied (Au, Ag, and AuAg alloy), the same trend is observed: the wavelength of the SPR peak decreases with temperature, from 670 nm for deposition at 200 °C down to 620 nm for deposition at 600 °C for Au, from 575 to 530 nm for Ag, and from 620 to 575 nm for AuAg alloys. Such a blue-shift is in coherence with the roughness increase[10] observed by AFM. During further immersion in biological media, Ag films were found to remove from the substrates except for deposition at 600 °C. To increase Ag adhesion, a thin film of $BaTiO_3$ was intercalated between the quartz substrate and the silver film. This sufficiently strengthened Ag adhesion to achieve satisfactory further CL experiments, while the presence of $BaTiO_3$ induced a red-shift of the SPR band (from 530 to 620 nm for the film deposited at 600 °C). All characteristics of the films studied are indicated in Table 1. Roughness is defined, using AFM, as the standard deviation of the height value within a box cursor with a size of 250 nm × 250 nm and a resolution of 256 pixels × 256 pixels. The specific area of gold, which depends on roughness, is evaluated from the average diameter, D, and the height, h, of the clusters. Compared with flat surfaces, the specific area of a rough film increases by a factor of Kh/D where K is a dimensionless coefficient, depending on the exact geometry of the clusters and is close to 2. This factor is denoted "surface area ratio" in Table 1. The different preparations allowed i) the variation of the distance between the luminol emission peak at 425 nm and the position of the plasmon band to a large extent (from 105 nm for the Ag film prepared at 600 °C to 245 nm for the Au one prepared at 200 °C) and ii) the obtaining of three chemically different samples (Au, Ag, AuAg alloys), with all of them having their plasmon absorption peaking at 620 nm (Fig. 2 right and Fig. 4c). The 620 nm position lies far from luminol emission (425 nm), so that the low overlap resulting between SPR and dye luminescence should limit plasmon assistance to CL enhancement. Then, if strong differences are evidenced in CL between all the metals investigated, it should be concluded that SECL clearly originates from catalytic mechanisms.

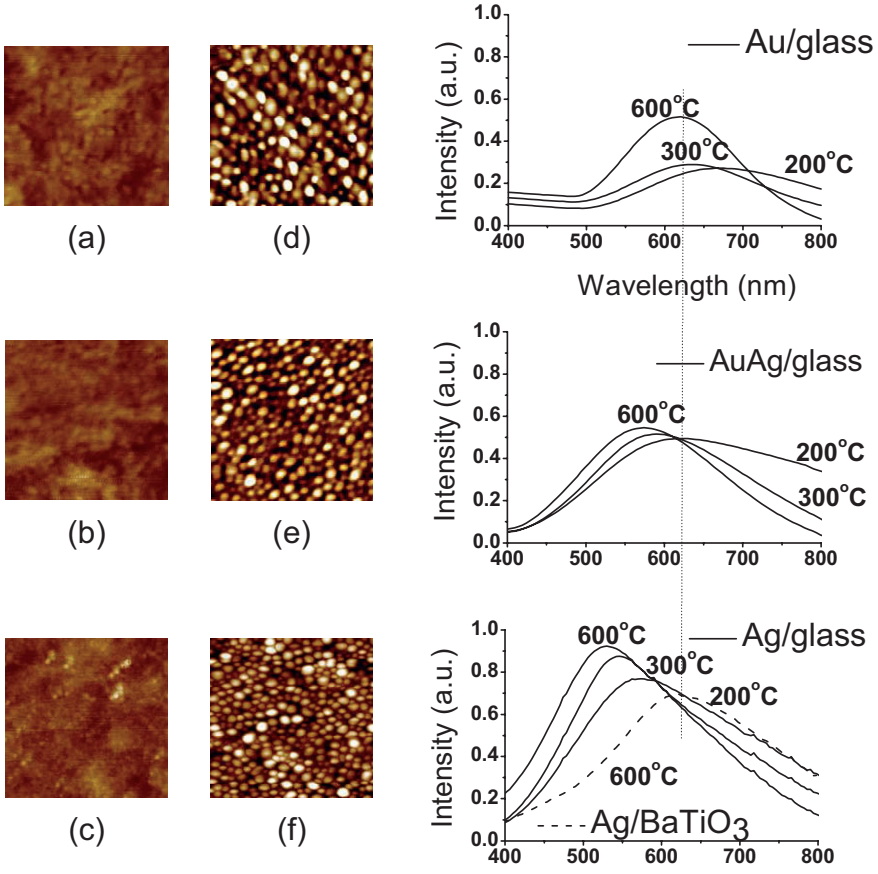

Figure 2. Left: AFM images (500 nm × 500 nm area) of "bulklike" Au (a), AuAg (b), and Ag (c) films prepared at room temperature, and "clusterlike" Au (d), AuAg (e), and Ag (f) films prepared at high temperature. Right: Extinction spectra of different "clusterlike" films (Au (upper graph), AuAg (middle), and Ag (lower)) deposited on glass at 200, 300, and 600 °C. The extinction spectrum of a "clusterlike" film of Ag deposited on a $BaTiO_3$-coated glass substrate at 600 °C is shown as the dashed line of the lower graph.

These metal films were used as chip substrates for luminol–H_2O_2 induced CL according to a process described in Figure 1 and already reported in our previous work.[4] In brief, trithiolated polypeptides modified with a biotin molecule at their N-terminal end were first spotted in 1.2 nL drops (1 mg mL^{-1}) on the films, through an automatic piezoelectric spotter. The peptides were incubated for 2 h and then washed to remove all unbound

ADVANCED FUNCTIONAL MATERIALS

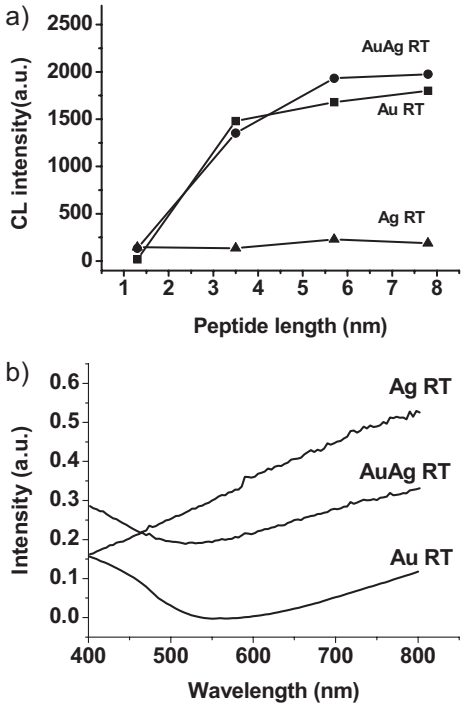

Figure 3. a) Luminol–H_2O_2 CL induced by peroxidase on bulklike Au, Ag, and AuAg alloy films for different metal–peroxidase distances. b) Extinction spectra of bulklike Au, Ag, and AuAg alloy films.

molecules. In the second step, the treated films were immersed for 20 min in veronal-buffered saline (VBS) containing an additional 1 % bovin serum albumin (BSA) and 0.1 % polyoxyethylenesorbitan monolaurate (Tween 20), and finally the films were incubated with peroxidase-labeled streptavidin (1 μg mL^{-1}) for 30 min. The peroxidase-labeled streptavidin has a globular size of 6–10 nm, and the distance between peroxidase and metal is adjusted by the peptide chain length. Four different peptides, corresponding to 5, 11, 17, and 23 amino acids and denoted P5, P11, P17, and P23, were used to get separation distances, *d*, of about 1.3, 3.5, 5.7, and 7.8 nm, respectively. The efficiency of peptide grafting on the different films was evaluated by X-ray photoelectron spectroscopy (XPS), which allowed the surface atomic ratios to be determined: S/M, N/M, N/S, and Au/Ag (where M represents metal; Table 2). One can assume that the metal depth analyzed in XPS is given by the product: λ [M], where λ is the inelastic mean free path of the photoelectrons ($\approx$ 5 nm for Au and $\approx$ 10 nm for Ag)[11] and [M] is the atomic metal concentration found by XPS. The peptide density can then be easily obtained from the metal density (59.0 atoms nm^{-3} for Au and 58.7 atom nm^{-3} for Ag), taking into account that each peptide contains four S atoms. Whatever the film, the peptide density lies between 1 and 4 peptide nm^{-2}. This density is lower than that normally obtained for monothiolate grafting on a flat Au(111) surface,[12] which is 5 thiols nm^{-2}. This can be easily explained by the higher steric hindrance of the trithiolated peptides used here.

Different conclusions can be drawn from the values given in Table 2. First, the grafting density on gold is the same whatever the nature of the film, bulklike or clusterlike (for P11 grafting, the density is 1.3 peptide nm^{-2} on a flat surface and 1.6 peptide nm^{-2} on a rough one). Second, as expected from increasing hindrance, the peptide density slightly decreases with the peptide length: from 2 peptide nm^{-2} for P5 to 0.9 peptide nm^{-2} for P23, when grafted on a gold film made at 600 °C. Third, the grafting density is higher on films containing silver than those made from pure gold.

XPS was also performed to characterize the grafting of streptavidin-labeled peroxidase on biotinylated peptides. After reaction of the 6–10 nm sized peroxidase on the trithiolated peptides, the metal becomes quasi-undetectable whatever the film and the peptide used. This indicates that for all films, the peroxidase continuously coats the surface. This result could be already inferred from the peptide densities evaluated by XPS. Because of the high affinity of streptavidin for biotin and the fact that a biotinylated site is available at positions every nanometer apart or less, whereas streptavidin-labeled peroxidase has a size of 6–10 nm (see Table 2), all the peptide densities are indeed sufficient to ensure a homogeneous peroxidase coating. In accordance with the literature,[13] this peroxidase coating induces significant modifications to extinction spectra (Table 3): a red-shift, a broadening, and a height increase of the plasmon peak. The red-shift slightly increases with the peptide length (from 24 nm for P5 to 30 nm for P23, when grafted on a gold film made at 600 °C) and is greater for silver than for gold (44 vs. 29 nm when peroxidase is grafted via P11). The sensitivity of the SPR to changes in the surrounding environment of the metal depends only slightly on the nature of the metal.[14] Thus, the greater red-shift in the case of Ag could be explained by the greater density of peptides grafted.

CL measurements were taken with a –30 °C cooled charge-coupled device (CCD) camera (Intelligent Dark Box II, Fuji Film). For this, the samples were dipped into a VBS solution containing luminol and additives that favored its biocatalyzed CL (220 μM luminol, 500 μM

Table 1. Characteristics of the samples studied. "Surface area ratio" is the ratio between specific areas of rough and flat films.

Film	Temperature [°C]	SPR position [nm]	SPR HWHM [nm] [b]	SPR intensity	Roughness [nm]	Particle size [nm]	Surface area ratio
Au	30	n.p. [a]	n.p.	n.p.	0.3	–	1
	600	620	72	0.42	1.9	~35	1.2±0.1
AuAg	30	n.p.	n.p.	n.p.	0.4	–	1
	200	620	150	0.46	4.0	27	1.2±0.1
	400	582	80	0.52	4.3	30	1.3±0.1
	500	576	60	0.61	4.4	32	1.3±0.1
Ag	30	n.p.	n.p.	n.p.	0.3	–	1
	600	530	123	0.84	3.1	35	1.3±0.2
Ag on $BaTiO_3$	600	620	130	0.70	3.6	37	1.35±0.2

[a] n.p.: No peak. [b] HWHM: Half width at half-maximum.

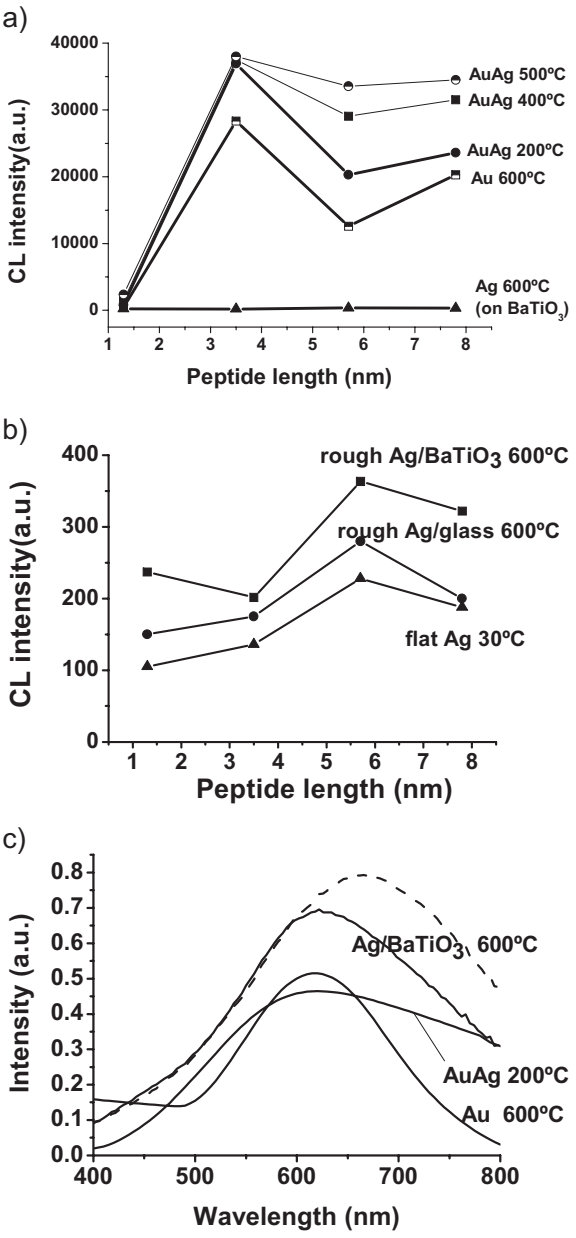

Figure 4. a) Luminol–H_2O_2 CL induced by peroxidase on clusterlike Au, Ag, and AuAg alloy films prepared at different temperatures with different metal–peroxidase distances. b) Luminol–H_2O_2 CL of different clusterlike Ag films. c) Extinction spectra (all peaking at 620 nm in the absence of a biological coating) corresponding to the wider solid CL curves of Au, Ag, and AuAg films: solid lines correspond to films without a biological coating; the dashed line corresponds to the Ag film coated by peroxidase-labeled streptavidin grafted via P11.

H_2O_2, and 200 μM *p*-iodophenol). The light emitted by the luminol in the vicinity of the peroxidase was integrated for 10 s. The images obtained were quantified and the results were given in arbitrary units (a.u.), each value being an average of four measurements. Figure 3b, which displays luminol CL in the vicinity of "bulklike" metal films, shows that Au and AuAg films on the one hand and Ag films on the other hand present two different behaviors. For Au and AuAg films, the CL intensity increases with distance and reaches a value of about 2000 in arbitrary units (a.u.). This behavior can be easily explained by metal quenching, which is efficient only below a critical metal–luminol distance comprised between 5 and 10 nm (luminol: the donor, metal: the acceptor).[15] Here CL quenching is negligible when the peptide length is longer than ≈3.5 nm, that is, for metal–peroxidase distances larger than ≈6 nm. This value of 6 nm, necessary to avoid luminol quenching, is then in good agreement with the order of magnitude for the critical donor–acceptor distance (5–10 nm). The behavior of the bulklike silver film is completely different: It can be noticed that compared with Au and AuAg alloy films: i) metal quenching is less pronounced and ii) the CL measured is one order of magnitude smaller for the longer peptide lengths. The first observation could be consistent with the greatest peptide density evidenced by XPS in the case of Ag. Indeed, at short distances, quenching is very sensitive to distance (in the Förster transfer theory it possesses an inverse fourth power dependence with this parameter)[15] so that the small increase in metal–peroxidase distance induced by a greater peptide density could be sufficient to significantly decrease quenching. Even if the spacer size is less than 2 nm, the effect of increasing density should be similar to that recently obtained when using single-strand DNA (ssDNA) molecules as spacers.[16] The second observation could be a first indication that the nature of the mechanism responsible for CL enhancement in the vicinity of corrugated surfaces could be catalytic and not plasmonic. Indeed, whereas the three films do not possess any SPR peak, they all present a small corrugation of the order of 0.3–0.4 nm, sufficient to ensure some CL catalysis if this mechanism is effectively involved in SECL. This would then indicate that nanometer-scale corrugated gold is a better catalyst than silver.

Figure 4a displays the CL signal relative to Au (deposited on glass at 600 °C), Ag (deposited on $BaTiO_3$ at 600 °C), and AuAg (deposited on glass at 200 °C) clusterlike films, which all possess an SPR peak at the same wavelength (620 nm) in the absence of a biological coating. Compared to flat films, Au and AuAg films present quite different behavior. For Au and AuAg films, the CL intensity first increases strongly with peptide lengths between 1.3 and 3.5 nm and then slowly decreases after 3.5 nm. For a peptide length of 3.5 nm (P11) the intensity reaches high values (around 30 000 in arbitrary units). XPS showed that flat and rough surfaces possess the same number of peroxidase molecules per unit area (Table 1). Also the difference in specific area between both kinds of surfaces is less than 20 % (Table 2). Therefore, this increase of more than one order of magnitude compared to the CL intensity found for flat films demonstrates that CL is effectively greatly enhanced by the presence of a corrugated metal. More precisely, the particular evolution of the CL signal can be explained on the basis of two competing phenomena: quenching and CL enhancement, each having a specific dependence on the luminol–metal distance.[17] At short distances, quenching, which is characterized by a rapid decrease with distance (Fig. 3), predominates so that the CL is low. When the distance is increased, quenching is negligible for peptide lengths longer than 3.5 nm (P11), so that, at long distances, the enhancing mechanism almost exclusively

ADVANCED FUNCTIONAL MATERIALS

Table 2. Atomic ratios (as determined by XPS), metal concentration ([M]), peptide density, and average distance between adjacent peptides.

	N/S		N/M	S/M	Au/Ag	[M]	Peptide density [peptide/nm^2]	Average distance [nm]
	theo	exp						
Flat Au P11		3.9±0.8	0.35±0.07	0.09±0.02	–	0.20±0.02	1.3±0.4	0.9±0.03
Rough Au P5	2.25	2.2±0.4	0.28±0.06	0.13±0.03	–	0.21±0.02	2.0±0.6	0.7±0.2
Rough Au P11	4.5	4.2±0.8	0.45±0.09	0.11±0.02	–	0.20±0.02	1.6±0.5	0.8±0.2
Rough Au P17	7.25	6.1±1.2	0.49±0.1	0.08±0.02	–	0.18±0.02	1.1±0.4	0.9±0.3
Rough Au P23	9.75	7.0±1.4	0.49±0.1	0.07±0.02	–	0.17±0.02	0.9±0.3	1.0±0.3
Rough Ag P5		2.2±0.4	0.37±0.08	0.27±0.06	–	0.10±0.01	4.0±1.2	0.5±0.2
Rough Ag P23		7.2±1.4	1.01±0.2	0.14±0.03		0.09±0.01	1.9±0.6	0.7±0.2
Rough AuAg P5		2.4±0.4	0.34±0.07	0.19±0.03	1.1±0.2	0.15±0.02	3.1±0.9	0.6±0.2

governs the CL dependence. The enhancement is then found to be characterized by a smoother decrease with distance. These two competing mechanisms explain the presence of a maximum for a peptide length of 3.5 nm, a value very close to the critical peptide length, above which quenching becomes negligible.

Again, the luminol CL behavior in the vicinity of clusterlike Ag films completely differs from that observed in the vicinity of Au or AuAg alloy ones. Whereas corrugation leads to an enhancement of more than one order of magnitude for Au and AuAg, it leads to an increase of only 50 to 100 % for Ag. This (relatively) low increase is consistent with that already reported by Aslan et al., who studied differently colored CL reagents.[2] Even if coating induces some SPR red-shift, it does not modify the extinction spectrum at low wavelengths. Figure 4c shows, for instance, that in the case of the Ag film deposited on $BaTiO_3$, spectra before and after peroxidase deposition are rigorously the same between 400 and 600 nm. For the films studied, the overlap between the metal SPR (645–670 nm, depending on the nature of the metal and more slightly on the peptide used) and luminol emission (425 nm) is almost negligible. The large difference between the enhancements observed for Au and Ag biochips indicates then that mechanisms other than plasmon-assisted processes should be involved in SECL. Also, if plasmons were still exerting some influence upon the CL, the enhancement should vary in a similar way to the SPR intensity (more important for Ag); this is not the case. The conclusion that CL is not enhanced by the presence of a metal plasmon is even clearer when one compares the two Ag films made at 600 °C on bare glass and on glass coated by $BaTiO_3$ (Fig. 2). These two samples differ strongly by the position of their SPR (530 and 620 nm in the absence of a coating) and then by their overlap with luminol emission (not modified by a coating). The localized plasmon of the clusterlike Ag film deposited on glass is at a distance of 105 nm from the luminol emission, whereas that of the film deposited on $BaTiO_3$ is at a distance approximately twice that (195 nm). However, the sample having the largest overlap with luminol emission (and which also has the higher plasmon intensity) is the one that presents the smaller enhancement (20 % instead of 60 % when P17 is chosen as the spacer between metal and peroxidase). All these results demonstrate an absence of correlation between SECL and the overlap between luminol emission and SPR: as stated by Zhang et al.,[3] the nature of the main mechanisms responsible for SECL must be catalytic.

CL is consecutive to luminol oxidation into a luminol radical. Two main mechanisms for catalysing this oxidation can be proposed. The first mechanism can be inferred from the apparent contradiction that catalysis involves contact interaction occurring at distances up to 1 nm whereas the CL enhancement is evidenced here for metal–peroxidase distances largely greater (around 10 nm). As the oxidation is known to proceed in two steps:[18] one involving peroxidase (and then taking place in close contact with it), and the other involving the presence of an oxygen-related radical (and then not necessarily required to append in close proximity to the peroxidase); it is this latter step that is most certainly catalysed by the presence of corrugated gold.[19] This interpretation was already proposed[3] to explain that enhanced electron transfer from gold clusters to adsorbed H_2O_2 (a process known as particle-mediated transfer) permitted to produce the key intermedi-

Table 3. Evolution of extinction spectra with biological coating for three films: Au, AuAg, and Ag/$BaTiO_3$. The coatings consist of peroxidase-labeled streptavidin grafted on metal via different peptides (P5, P11, P17, and P23).

Film	Type of coating	SPR position [nm]	SPR HWHM [nm]	SPR intensity
Au, 600°C	No coating	620	72	0.42
	P5	644	83	0.46
	P11	649	83	0.45
	P17	652	85	0.52
	P23	650	87	0.49
AuAg, 200°C	No coating	620	150	0.46
	P11	657	169	0.53
Ag/$BaTiO_3$,	No coating	620	130	0.70
600°C	P11	664	150	0.79

ate hydroxy and hydroperoxide radicals,[20] which leads to the enhancement of CL. It requires that the CL reagents can pass the biological layer whatever the peptide density, which is justified by the absence of correlation between CL intensity (Fig. 4) and peptide density (Table 2). The second mechanism, acting in conjunction with the first one, could arise from a decrease of the redox potential of luminol in the vicinity of the corrugated gold. Such a shift, which facilitates luminol oxidation in the presence of catalysing peroxidase, was already evidenced by our team when luminol was directly fixed on a gold cluster.[21] In any case, the catalytic enhancement arises from the modification of thermodynamic properties near highly curved surfaces[22] and is expected to increase with roughness for all the metals investigated here. This correlation was already observed in the case of gold,[4] for which CL increased by 25 % when roughness increased from 1.3 to 1.9 nm. It is now verified for AuAg alloys: when peroxidase is fixed via P23, CL increases more than 50 % for a roughness increase from 4.0 to 4.4 nm. It is finally also verified for Ag: the increase of Ag roughness induced by a previous deposition of $BaTiO_3$ (from 3.1 to 3.6 nm) leads to a CL increase of around 30 %.

A correlation between SPR intensity and CL enhancement has already been pointed out in the literature.[3] Figure 5 shows that, in fact, such correlations can be found within each metal family (Au, Ag, or AuAg alloy) but can not lead to a universal rule that would be valid regardless of the nature of the metal. The reason that such a correlation can be established within each kind of metal is that SPR intensity and SECL have a similar evolution with roughness. Roughness increases the number of localized electrons responsible for strong Mie resonances. It also increases the film curvatures responsible for increased catalytic activity. Then, whereas localized SPR intensity is an indicator of the number of metal electrons liable to catalyse CL,[23] the efficiency of the catalysis depends on the chemical nature of the metal.

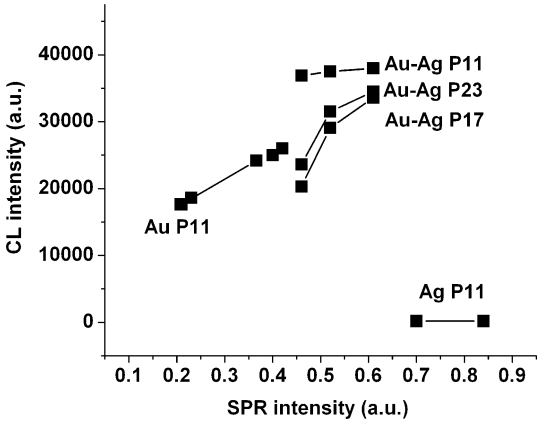

Figure 5. Relationship between the CL and SPR intensities for metal families that differ in their composition: Au, Ag, and AuAg alloys. Within a family the different points correspond to different corrugations (and, for Au, to different peptide graftings).

3. Conclusions

A large number of samples, in which the chemical nature of the film and the position of the SPR peak were independently varied, were fabricated to discriminate between the two possible SECL mechanisms a priori. This allowed plasmon-assisted processes to be eliminated as the main mechanisms responsible for SECL. Indeed, the metal with the strongest plasmon resonance (Ag) is the one that also induces the smallest CL enhancement. The CL enhancement was then related to catalytic mechanisms, the efficiency of which is governed by a key parameter, the roughness. In this context, nanoscale-corrugated gold appears as a better catalyst than silver for surface-enhanced CL. These results allow the further optimization of biochips either by using metals, such as palladium or platinum, known for their strong catalytic properties or by optimization of the structure's roughness.

4. Experimental

Fabrication of Metal Films: The noble-metal films used in this paper were all prepared on quartz substrates with a pulsed-laser deposition (PLD) technique under vacuum (~ 10 Pa). In the homemade apparatus, a foil of the compound to be deposited (used as a target) was placed at a distance of about 40 mm from the quartz substrate. An XeCl excimer laser (308 nm full width at half-maximum, 17 ns) operating at a 1 Hz repetition rate was then focused onto the target. Two main factors can be used to easily control the properties of the metal films: the film thickness and the substrate temperature during deposition. Commonly, noble-metal films can change from a clusterlike material to a bulklike one with increasing thickness; this is accompanied by red-shifting of the surface plasmon resonance band accordingly before finally disappearing. Also, the metal film can change from a bulklike material to a clusterlike one when the deposition substrate temperature is increased: this is correlated to the appearance of an SPR band followed by a further blue-shift, as shown in previous work [24]. Therefore, Au and Ag thin films with various properties can be easily prepared using a PLD technique by controlling either the deposition thickness or the temperature. In our experimental conditions, the thickness was kept constant and the temperature was the tunable parameter. Additionally, before the Ag film was deposited, a 1 nm thick $BaTiO_4$ layer was deposited onto the quartz substrate to enhance the adhesion between the Ag film and the substrate. Furthermore, the AuAg alloy films were prepared using the target technique. A disk target that can rotate in plane was made of Au and Ag fan-shaped foils, the Au/Ag ratio of alloy films being controlled by adjusting the fan-shaped area ratio.

X-ray Photoelectron Spectroscopy: XPS analysis of the films before and after deposition of biomolecules, such as peptides, was carried out at the Institut de Recherche sur la Catalyse (IRC) with a VG Scientific ESCA LAB 200 R instrument with 220 W Al Kα radiation (1486.6 eV). Spectra relative to C 1s, O 1s, N 1s, S 2p, Si 2s, Au 4f7/2, and Ag 3d photoelectron peaks were measured at binding energies around 284.6, 531.0, 399.4, 162.8, 153.3, 83.7, and 367.9 eV, respectively. The spot size on the sample was of 400 μ × 1000 μ. The areas of the elements' peaks allowed the atomic ratio to be calculated according to the following formula (the example shown here is for N and S):

$$\frac{S}{N} = \frac{k_n}{k_s} \cdot \frac{\text{area(S)}}{\text{area(N)}} \quad (1)$$

where k_S and k_N are the S and N sensitivity factors.

Sensitivity factors contain the photoemission cross sections as approximated from a Hartree–Slater atomic model. With the ESCA

ADVANCED FUNCTIONAL MATERIALS

LAB 200 R instrument, the factors are corrected by a factor proportional to $E_{kin}^{0.1}$ (where E_{kin} is the kinetic energy) Attenuations from the free electron mean path and from the transfer function of the spectrometer are then accounted for. As a consequence, from all the above approximations, absolute uncertainties in XPS quantitative analysis are generally of the order of ± 10 % in magnitude.

Atom Force Microscopy: AFM images of films were collected using a Digital Instruments Nanoscope Di3100 microscope operated in the tapping mode.

Absorption: The metal films were characterized by optical absorption measurements made at room temperature from 200 to 1500 nm using a Lambda 9000 Perkin–Elmer spectrophotometer. All spectra were collected in standard transmission geometry with unpolarized light. The probe beam diameter was 1 mm.

Received: December 7, 2006
Revised: February 16, 2007
Published online: July 12, 2007

[1] K. Aslan, C. D. Geddes, *Anal. Chem*. **2005**, *77*, 8057.
[2] K. Aslan, S. N. Malyn, C. D. Geddes, *J. Am. Chem. Soc*. **2006**, *128*, 13 372.
[3] Z. F. Zhang, H. Cui, C. Z. Lai, L. J. Liu, *Anal. Chem.* **2005**, *77*, 3324.
[4] G. W. Lu, B. L. Cheng, H. Shen, Z. H. Chen, G. Z. Yang, C. A. Marquette, L. J. Blum, O. Tillement, S. Roux, G. Ledoux, A. Descamps, P. Perriat, *Appl. Phys. Lett.* **2006**, *88*, 023 903.
[5] M. Moskovits, *Rev. Mod. Phys.* **1985**, *57*, 783.
[6] A. Otto, *J. Raman Spectrosc.* **2005**, *36*, 497.
[7] J. Lee, A. O. Govorov, J. Dulka, N. A. Kotov, *Nano Lett*. **2004**, *4*, 2323.
[8] G. Yang, W. T. Wang, Y. L. Zhou, H. B. Lu, G. Z. Yang, Z. H. Chen, *Appl. Phys. Lett*. **2002**, *81*, 3969.
[9] U. Kreibig, M. Vollmer, in *Optical Properties of Metal Clusters*, Springer, Heidelberg, Germany **1995**, Ch. 2.
[10] M. C. Daniel, D. Astruc, *Chem. Rev.* **2004**, *104*, 293.
[11] M. P. Seah, W. A. Dench, *Surf. Interface Anal*. **1979**, *1*, 2.
[12] L. H. Dubois, R. G. Nuzzo, *Annu. Rev. Phys. Chem.* **1992**, *43*, 437.
[13] D. A. Stuart, A. J. Haes, C. R. Yonzon, E. M. Hicks, R. P. Van Duyne, *IEE Proc. Nanobiotechnol.* **2005**, *152*, 13.
[14] K. S. Lee, M. A. El-Sayed, *J. Phys. Chem. B* **2006**, *110*, 19 220.
[15] W. L. Barnes, *J. Mod. Opt.* **1998**, *45*, 661.
[16] E. Dulkeith, M. Ringler, T. A. Klar, J. Feldmann, A. Munoz Javier, W. J. Parak, *Nano Lett*. **2005**, *5*, 585.
[17] G. W. Lu, H. Shen, B. Cheng, Z. Chen, C. A. Marquette, L. J. Blum, O. Tillement, S. Roux, G. Ledoux, M. G. Ou, P. Perriat, *Appl. Phys. Lett*. **2006**, *89*, 223 128.
[18] C. A. Marquette, L. J. Blum, *Rec. Res. Dev. Pure Appl. Anal. Chem*. **2002**, *4*, 9.
[19] R. Grisel, K. J. Weststrate, A. Gluhoi, B. E. Nieuwenhuys, *Gold Bull*. **2002**, *35*, 39.
[20] A. J. Henglein, *J. Phys. Chem*. **1993**, *97*, 5457.
[21] S. Roux, B. Garcia, J. L. Bridot, M. Salomé, C. Marquette, L. Lemelle, P. Gillet, L. J. Blum, P. Perriat, O. Tillement, *Langmuir* **2005**, *21*, 2526.
[22] J. Gibbs, *Collected Works*, Yale University Press, New Haven, CT **1928**.
[23] S. Link, M. A. El-Sayed, *Int. Rev. Phys. Chem*. **2002**, *19*, 409.
[24] G. Lu, B. Cheng, H. Shen, Y. Zhou, Z. Chen, G. Yang, O. Tillement, S. Roux, P. Perriat, *Appl. Phys. Lett.* **2006**, *89*, 223 904.